Combined LIBS and Acoustics for Differentiating Minerals with Similar LIBS Spectra

J. Laserna, C. Alvarez-Llamas, P. Purohit, J. Moros, S. Luna, A. Jurado, F. J. Lopez, Roger Wiens, Sylestre Maurice, Olivier Gasnault, et al.

COMBINED LIBS AND ACOUSTICS FOR DIFFERENTIATING MINERALS WITH SIMILAR LIBS SPECTRA J. Laserna[1], C. Álvarez[1], P. Purohit[1], J. Moros[1], S. Luna[1], A. Jurado[1], F.J. López[1], R.C. Wiens[2], S. Maurice[3], O. Gasnault[3], O. Beyssac[4], N. Lanza[2], A. Ollila[2], J. Lasue[3], E. Gibbons[6], T. Fouchet[7], R. Lorenz[5], D. Mimoun[8], G. Delory[9], X. Jacob[8], N. Murdoch[8], B. Chide[3], C. Legett[2], D. Delapp[2], P. Pilleri[3], R. Perez[3], P. Bernardi[7] and G. Lacombe[10] ([1]U. Malaga, Spain; laserna@uma.es; [2]LANL, Los Alamos, NM; [3]IRAP, Toulouse, France; [4]IMPMC, Paris, France; [5]APL/JHU, Laurel, Maryland; [6]McGill, Montreal, Canada; [7]LESIA, Paris, France; [8]ISAE-SUPAERO, Toulouse, France; [9]UC Berkeley, Berkeley, CA; [10]UVSQ, Versailles, France)

Introduction: The SuperCam remote sensing instrument suite onboard the Perseverance rover for NASA's Mars 2020 is qualified to perform laser-induced breakdown spectroscopy (LIBS), remote Raman spectroscopy, visible and infrared (VISIR) reflectance spectroscopy, acoustic sensing and high resolution color imaging. The architecture of this multipurpose instrument is due to the imperative need to cross-validate the responses of the involved analytical techniques in order to define the mineralogy of Martian rocks and soils with high accuracy. So far, owing to the complementary nature of data from LIBS and Raman spectroscopy, these approaches have been exploited using data fusion algorithms for an improved categorization of minerals [1–4]. However, the different experimental conditions required for each phenomena to emerge imply that the spectral information usually derives from sequential laser pulses that do not necessarily derive from the same target area. In consequence, advantages of data fusion strategies cannot be fully exploited, as the sources of the merging information must belong to the same entity. The SuperCam toolkit integrates a microphone that intends to listen to the sound wave linked to the shockwave created by the supersonic expansion of plasmas generated when the sampling laser hits rocks several meters away from the Perseverance rover [5–7]. In this case, the correspondence of LIBS with the acoustic wave is assured. Therefore, data merging may result in richer and unique data sets that can be used for differentiating unknown rocks and mineral assemblages benefitting from the complementary information provided by acoustics and LIBS, while keeping the spatial resolution of laser ablation.

Samples: Six iron minerals were considered because of the difficulty in identifying them solely on the basis of their LIBS fingerprint: ferric oxides –hematite (Fe_2O_3) and magnetite ($Fe^{2+}Fe^{3+}{}_2O_4$)–, ferric oxyhydroxides –goethite (α-$Fe^{3+}O(OH)$ and limonite ($FeO(OH)\cdot nH_2O$)–, iron-sulfide pyrite (FeS_2) and iron carbonate siderite ($FeCO_3$). All the minerals, originally in their natural form, were cut and conveniently polished to avoid alteration of the acoustic signal attributable to morphological surface irregularities.

Instrument Description: Experiments herein were conducted inside an environmental simulation chamber able to mimic the atmosphere conditions of Mars. The excitation source, located outside the chamber, consisted of a pulsed Nd:YAG laser (1064 nm, 10 Hz, pulse width 4 ns). Laser pulses were first expanded with a beam expander and then guided into the chamber through a vacuum viewport window using a mirror. Once inside, laser pulses were redirected to and focused on samples by a mirror and a lens, respectively. This optical configuration led to a spot diameter of ca. 250 μm at the target surface when located at about 2 meters away from the lens. The batch of samples –with their polished surface oriented towards the laser propagation axis– was placed on the platform of a X linear motorized stage that allowed changes in the sampling position. The sample holder was housed inside a custom-built hemi-anechoic chamber (70×40×40 cm^3, L×W×H).

For capturing sounds from laser-induced breakdown, a 6 mm pre-polarized condenser microphone (20 Hz–19 kHz frequency response, omni-directional polar pattern, 14 $mV.Pa^{-1}$ sensitivity) was used. The microphone was enclosed within a custom hemi-anechoic tubular chamber (50×20 cm L×D). This acoustic suite was quasi-coaxially positioned to the direction of plasma expansion – an angle of about 10˚ was used to-overcome possible obstruction of the focusing lens– at a fixed sample surface-to-microphone distance of 200 cm. A 24-bit/192 kHz audio interface (UA-55 Quad-capture, Roland) was used at sampling rate of 96 kHz for digitalization of acoustic waves. Audacity was used to record the audios.Simultaneously with the audible events, light emitted by the plasmas was collected through a telescope. The optical emission detection system was coupled to the tip of a 2-m long bifurcated fiber optic cable - 2×600 μm core. The plasma light was guided to the entrance of a multi-channel miniature 75-mm focal length Czerny-Turner spectrograph with CCD detection. Under this configuration, LIBS spectra ranging from 235 nm to 595 nm were obtained. Temporal settings to gather the plasma light were 1.1 ms gate width and 0 μs delay. A total of 300 plasmas were analyzed for each sample (100 plasma events per position at 3 different positions along the surface of the mineral).

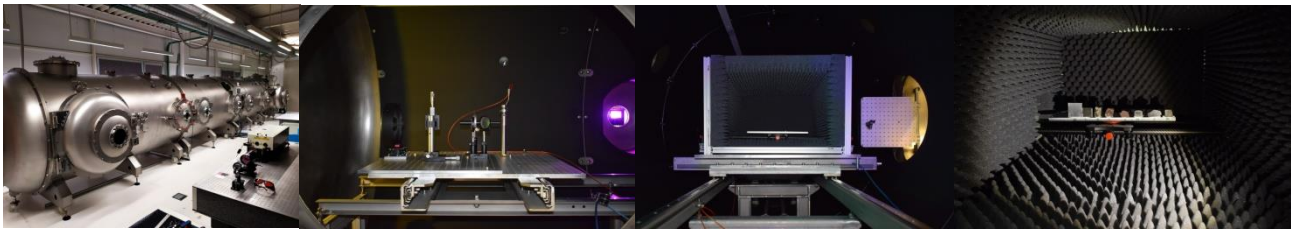

Fig. 1. From left to right: planetary environment simulation chamber; optical train for sending laser pulses and collecting the light from the plasmas and microphone for capturing the acoustic waves; anechoic chamber where the samples are housed; batch of iron minerals arranged for analysis.

Results: Principal component analysis (PCA) was performed using the normalized LIBS spectra to display any variation among the 6 minerals. The score plot is shown in Figure 2. The first three principal components explained 95% (PC-1: 84%, PC-2: 7% and PC-3: 4%) of the variations among total spectral information. Each point in the scatter plot represents one LIBS spectrum.

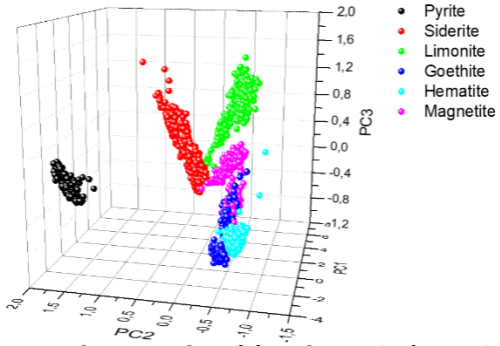

Fig. 2. The score plot of first three PCs from PCA on LIBS data of 6 iron-based minerals.

As shown, pyrite seems to be significantly different from the rest of the minerals, perhaps due to the absence of oxygen in its composition, rather than by its sulfur content. For the other 5 minerals, differences between LIBS signals are modest and are close to the variability exhibited by the intra- and inter-position LIBS intensities.These results were though expected due to the related LIBS spectra of the iron minerals analyzed. Similarly Figure 3 shows the score plot of the first three PCs from PCA on the normalized frequency power spectra derived from the acoustic waveforms. In this case, clusters corresponding to pyrite, siderite, limonite and magnetite are well differentiated in the graph, with the data reasonably well grouped for each mineral. However, Fig. 3 shows that the acoustic signals do not allow to separate goethite and hematite in two different clusters. Despite these good results, since the acoustic spectrum may be influenced by the size and shape of the target, studies to evaluate the effect of sample geometry and size on the frequency spectrum are ongoing.

However, a basic combination of the spectral outputs of the acoustic and LIBS sensors like the tensorial product of their two mormalized intensity vectors allows to create a new pattern (2D image) which clearly differentiates the minerals being considered.

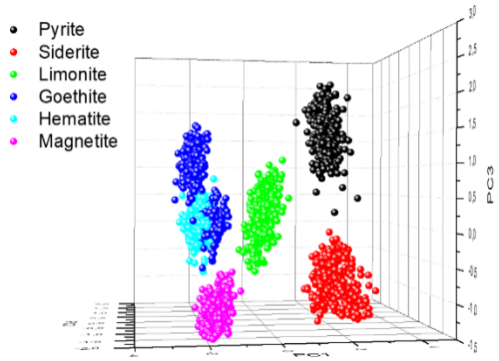

Fig. 3. The score plot of first three PCs from PCA on frequency spectra of laser-induced sound waves of 6 iron-based minerals.

Figure 4 shows the score plot of the first three PCs from PCA on the 2D images generated for each mineral. The scatter plot compares the three 2D images for each mineral coming from the averaged info gathered from each analized position. As seen, minerals are better differentiated through the fused data than by comparing exclusively the atomic or the acoustic spectral features by themselves.

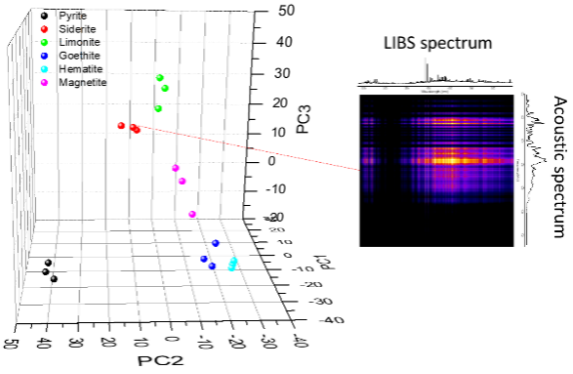

Fig. 4. The score plot of first three PCs from PCA on fused LIBS and acoustic data of 6 iron-based minerals. On the right, example of the 2D image generated from the fusion of the LIBS and acoustic information of the siderite ore

References: [1] Moros J. et al (2018) Anal. Chem. 90, 2079. [2] Rammelkamp K. et al. (2020) J. Raman Spectrosc. 51, 1682. [3] Manrique-Martinez J.A. et al. (2020) J. Raman Spectrosc. 51, 1702. [4] Gibbons E. et al. (2020) Spectrochim. Acta B 170, 105905. [5] Chide B. et al. (2019) Spectrochim. Acta B 153, 50. [6] Murdoch N. et al. (2019) PSS 165, 260. [7] Chide B. et al. (2020) Spectrochim. Acta B 174, 106000.